Agriculture, Ecosystems and Environment 240 (2017) 182–193

Contents lists available at ScienceDirect

Agriculture, Ecosystems and Environment

journal homepage: www.elsevier.com/locate/agee

Research paper

Quantifying and predicting spatio-temporal variability of soil CH_4 and N_2O fluxes from a seemingly homogeneous Australian agricultural field

M.D. McDaniel[a,b,*], R.G. Simpson[a], B.P. Malone[c], A.B. McBratney[c], B. Minasny[c], M.A. Adams[a]

[a] Centre for Carbon Water and Food, Sydney Institute of Agriculture, University of Sydney, Camden, New South Wales 2570, Australia
[b] Department of Agronomy, Iowa State University, Ames, IA, 50011, United States
[c] The Biomedical Building (ATP), Sydney Institute of Agriculture, University of Sydney, Sydney, New South Wales 2006, Australia

ARTICLE INFO

Article history:
Received 27 July 2016
Received in revised form 10 February 2017
Accepted 14 February 2017
Available online xxx

Keywords:
Agriculture
Dynamic chambers
Electromagnetic induction
Gamma radiometrics
Geospatial statistics
Greenhouse gas
Methane
Nitrous oxide
Proximal sensors
Spatial variability

ABSTRACT

Soil methane (CH_4) and nitrous oxide (N_2O) fluxes are difficult to predict from soil temperature and moisture alone, especially compared to carbon dioxide (CO_2) fluxes. That difficulty is reflected in high spatial and temporal (spatiotemporal) variability of these two greenhouse gases (GHGs). We used a 16 ha field, under homogeneous soils and vegetation, to simultaneously explore spatial and temporal variability of soil CH_4 and N_2O fluxes. We also measured soil physical and chemical properties in order to explain, and predict, spatial variability of these two gases. Gas fluxes were measured using either a dynamic chamber (spatial variability study) or automated chambers using FTIR (temporal variability study). Soil samples were analysed for 30 chemical parameters (including at least two forms of soil carbon and nitrogen), while two proximal soil sensors were used to collect fine-resolution soil electrical conductivity and gamma radiometric concentration across the site. Fluxes of CH_4 and N_2O showed distinct spatial patterns, and were uniquely related to soil properties. Spatial variability in both CH_4 and N_2O fluxes was greater than five months of temporal variability (an increase in 112% and 39% in standard deviations for each gas respectively). If we relied solely on the autochambers for mean field fluxes, we would have underestimated fluxes by 59 and 197%, for CH_4 and N_2O respectively. CH_4 fluxes were more spatially-dependent than those of N_2O (semivariance analysis), but both showed greater spatial dependence than previously reported. Nearly 40 and 50% of the mean spatial flux of CH_4 and N_2O were from 1% of the area. Spatial variability in soil CH_4 fluxes was predicted best by electrical conductivity measurements at 0–50 cm ($r = 0.74$) and soil C. Soil N_2O fluxes, on the other hand, were predicted best by soil N and the gamma radiometric data ($r = 0.48$). Overall, our results clearly show that the large spatial variance of both CH_4 and N_2O fluxes requires great caution when scaling from chamber-based measurements to the field and beyond. Proximal sensors (as used here) can help map "hot spots" of soil CH_4 and N_2O fluxes at the field scale.

© 2017 Elsevier B.V. All rights reserved.

1. Introduction

Research into greenhouse gas (GHG) fluxes has progressed rapidly in the last half century, and especially in the past decade. A unifying theme is that spatial and temporal (spatiotemporal) variability in soil GHG emissions can be so large as to obscure differences among land uses and treatments, leading to a still-urgent need to better-measure and understand that variability (Gregorich et al., 2005; Johnson et al., 2007; Kravchenko and Robertson, 2015). Progress is essential if we are to achieve site-specific management recommendations to reduce GHG emissions on managed land (Hénault et al., 2012; Paustian et al., 2016). Much of our understanding of spatiotemporal dynamics has been limited by technologies that restrict measurements to relatively small sampling areas and infrequent measurements through time. However, recent technological advances in GHG measurement and sampling technologies are offering the promise of rapid improvement in our understanding of the causes of variation.

Abbreviations: ATV, all-terrain vehicle; DOC, dissolved organic C; DON, dissolved organic N; EM, electromagnetic sensor; EC, electrical conductivity; GHG, greenhouse gas.

* Corresponding author at: Department of Agronomy, Iowa State University, 2517 Agronomy Hall, Ames, IA 50014, United States.
E-mail address: marsh@iastate.edu (M.D. McDaniel).

http://dx.doi.org/10.1016/j.agee.2017.02.017
0167-8809/© 2017 Elsevier B.V. All rights reserved.

The use of automated gas flux chambers (that allow continuous measurements of fluxes at intervals on the scale of minutes to hours), for example, has helped considerably improve our knowledge of the driving influences on temporal variability in soil GHG fluxes (Butterbach-Bahl et al., 1997; Pumpanen et al., 2003; Lai et al., 2012; Savage et al., 2014; Wang et al., 2011). Studies using these automatic(auto)-chambers have highlighted the importance of episodic events where soil GHG emissions are disproportionately large compared to "normal" conditions – also called "hot moments" (McClain et al., 2003; McDaniel et al., 2014). Missing these pulse events could underestimate annual emissions of carbon dioxide (CO_2) by up to 13% and nitrous oxide (N_2O) by 24%, and overestimate methane (CH_4) uptake by 18% in wheat-fallow cropping systems, for example (Kessavalou et al., 1998). Relatively high-frequency measurements with auto-chambers have substantially increased our knowledge of the "when, and why" of these "hot moments".

Spatial variability, on the other hand, remains a serious unresolved issue. Chambers, irrespective of whether they are automatic or manual, can only be used to measure fluxes from a small area (say up to 1 m^2 in area per chamber) relative to the size of typical paddocks or fields. Unfortunately, many studies have sought to extrapolate from such small areas to the field or even to the regional scale, despite obvious weaknesses and uncertainties associated with that scaling (Kravchenko and Robertson, 2015; Lessard et al., 1994; Velthof et al., 1996). A significant methodological limitation is the amount of time required to measure a flux from any single chamber (typically 30 min to 1 h), which precludes large-scale chamber deployments. While eddy flux and eddy gradient methods integrate fluxes over large areas (>500 m^2), they do not provide fine spatial resolution nor the ability to distinguish roles of differing soil processes that are known to control GHG emissions, and that likely varies at scales ranging from sub-micron to metres.

The recent advent of portable, quantum cascade, laser gas analysers, provides the ability to better-quantify spatial variability in GHG fluxes. Some laser analysers can measure gas concentrations at frequencies of 10–20 Hz, substantially reducing the time required to determine a soil flux (Hensen et al., 2006; Jassal et al., 2016). Faster 'turnaround' times can provide greater opportunity to increase the spatial density of GHG flux measurements. The ability to measure at high frequency has also led to 'dynamic' chamber methods (Hensen et al., 2006; Cowan et al., 2014). Dynamic chamber methods offer much more rapid assessment of fluxes and greater precision compared to traditional methods (Cowan et al., 2015; Hensen et al., 2006) and avoid problems associated with long deployments, such as, non-linear fluxes (Venterea et al., 2009).

Mounting evidence suggests that soil temperature and moisture alone are weaker predictors of CH_4 and N_2O fluxes than of CO_2 fluxes. More complex biological and chemical processes are involved in the former, and these processes are likely introducing greater spatial variability. It has been hypothesized that these soil biological and chemical properties should be more spatially variable than physical soil properties (Yanai et al., 2003). Indeed, soil properties such as soil carbon (Miller et al., 2016), nutrients (Mallarino, 1996), and microbial biomass and activity (Cambardella et al., 1994; Cavigelli et al., 2005) have shown considerable variability at the field-scale. Even soil water can vary greatly at the field-scale, and in relatively homogeneous landscapes (Longchamps et al., 2015). Each of these soil properties have been shown to contribute to regulation of CH_4 and N_2O fluxes, but have not been directly linked to spatial variability of GHG fluxes at the field scale.

We sought to determine the spatiotemporal variability of CH_4 and N_2O fluxes in a typical agricultural setting. We chose a field in Australia's northern wheatbelt, in northern New South Wales to simultaneously capture both spatial and temporal variability in these GHGs by using two systems: automated chambers for temporal variability, and dynamic chambers for spatial variability. Our objectives were to: 1) quantify and compare the spatial and temporal variability of CH_4 and N_2O fluxes in a 16 ha site, and 2) quantify soil properties that may be regulating this variability. We combined gas flux measurements with soil surveys using two proximal sensors and chemical analyses of soil samples. Proximal sensors are fast and easy to use, and can approximate several important soil variables that likely regulate soil fluxes of CH_4 and N_2O (see Materials & Methods section).

2. Materials & methods

2.1. Site description and experimental design

This study was conducted in a 16 ha section of a larger (~200 ha) field that forms part of the Plant Breeding Institute (149.8236483° E; 30.2778883° S) of the University of Sydney, at Narrabri, New South Wales, Australia. The institute lies at an

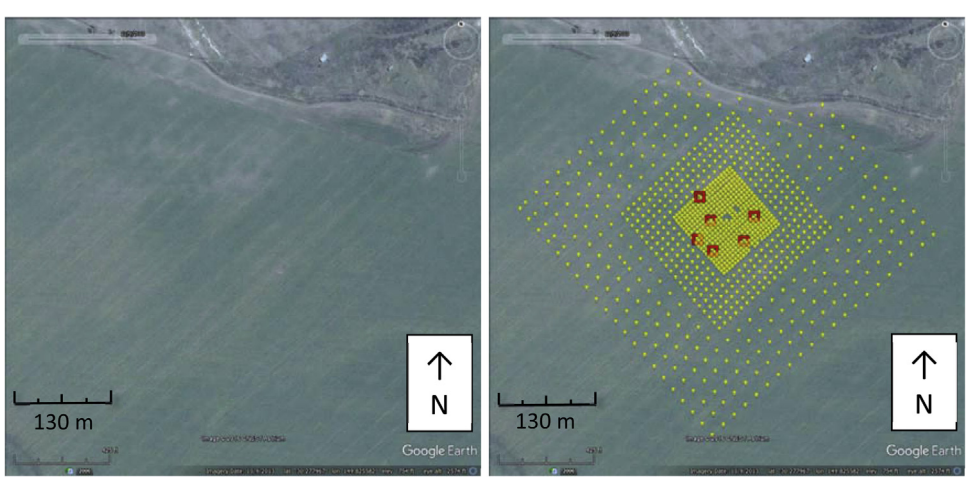

Fig. 1. Google Earth images of the study site without (left) and with (right) GPS locations of the autochambers for temporal variability (red squares) and spatial study sampling points (yellow markers). We used a dynamic chamber method to quantify rates of GHG emissions at points within three concentric squares. In the innermost 100 m x 100 m square, we sampled on a 5 m grid; in the concentric 200 m x 200 m square we sampled on a 10 m grid; while in the 400 m x 400 m concentric square, we sampled using a 20 m grid.

elevation of 232 m asl within a region known as the North-west Slopes and Plains and is drained by the Namoi River. Soils are mostly grey cracking clays (or vertisols by USDA classification), and the texture is 28% clay and 30% sand in the top 10 cm. The mean annual temperature for Narrabri is 19 °C, and mean annual precipitation is 662 mm.

We selected this site owing to its flat relief with an overall slope of just 1.8%. Historically, the field received fertilizer at rates of ~110 kg ha^{-1} y^{-1} as urea and has been used to grow wheat (*Triticum* sp.) and chickpea (*Cicer arietinum*) in rotation. We took our measurements after wheat harvest, with substantial residue remaining on the surface. For the spatial GHG study, we divided the 16 ha study site into three concentric squares with variable sampling densities within each square (Fig. 1). We sampled the central 100 m x 100 m square at 5 m intervals. We also sampled a concentric 200 m x 200 m square at 10 m intervals, and a 400 m x 400 m square at 20 m intervals.

2.2. Temporal variability in GHG fluxes

We placed six automated chambers (autochambers), roughly equidistant from each other within the central 100 m x 100 m of the study site. Autochambers were connected to a Fourier-transformed infrared (FTIR) gas analyser, capable of quantifying multiple gas species simultaneously. The FTIR was housed in a field-deployable, temperature-controlled enclosure and recorded concentrations of CO_2, CH_4, and N_2O (Griffith and Galle, 2000) according to a programmed sequence. Each chamber was within 50 m of the FTIR. Gases were sampled via a sample line (3/8" Synflex, Eaton Corporation), and opening/closing of the chamber was controlled pneumatically (via 6 mm nylon tubing; Norgren). GHG fluxes were calculated on the basis of changes in concentrations over a 45-min period during which the chamber lids were closed (see also Butterbach-Bahl et al., 1997 for description of similar sampling systems). A new sample from alternating chambers occurred every hour, thus the sampling interval for individual chambers was 6 h apart. The FTIR system was in place from February 12, 2015 until June 13, 2015.

2.3. Spatial variability in GHG fluxes

We employed a LGR N_2O—CH_4 Analyzer (Los Gatos Research, Mountain View, CA), coupled with a dynamic chamber to quantify spatial GHG fluxes. The LGR is a portable cavity ring-down spectroscopic analyser that measures N_2O, CH_4, and water vapour continuously at 1 Hz. The approximate flow of the internal pump in the analyser is 157 ml m^{-1}. The limit of detection for the LGR is 9 ± 1 ppb for N_2O and 47 ± 3 ppb for CH_4. The LGR was connected with 3.5 m of Synflex tubing to a square gas flux chamber made of PVC (dimensions 15 cm x 15 cm x 7.5 cm). We chose to use a smaller, dynamic chamber in order to quickly detect changes in GHG concentrations. In most cases, stable concentration data were obtained between 1 and 2 min after inserting the chamber 2.5 cm into the soil surface (Fig. S1). We deployed the chamber for a total of 5 min, with CH_4 or N_2O fluxes calculated on the basis of a linear function fitted to the data after the initial 1-to-2-min disturbance period (Fig. S1). Multiple measurements with manual, automatic, and the dynamic chamber all show strong linearity for fluxes measured between 2 and 45 min at this site. Therefore, we used linear regressions regardless of whether they exceeded the machine limit of detection in 5 min because it is very likely that these 2-to-5-min regressions would exceed this by 20–30 min if allowed. These measurements were all taken between the 23rd and 31st of May 2015 and tagged with a spatial reference coordinate using a GPS receiver (SMART6-L GNSS; NovAtel, Canada). Gas measurements were collected between sunrise and sunset and >100 such flux calculations were collected each day. The air and soil temperature varied little during this period, and there was no rain (Fig. S2).

2.4. Proximal soil sensing

We mapped soil properties using two proximal sensors (Table 1) on May 25th, 2015. The two proximal sensors we used in this study were a RSX–1 gamma radiometric detector consisting of a 4L Sodium-Iodine crystal (Radiation Solutions Inc., Mississauga, Ontario, Canada), and a Geonics DUALEM-21S electromagnetic induction instrument (Geonics Ltd, Mississauga, ON, Canada). Data from these instruments were logged continuously with measurements being taken approximately every 1 m assuming our average speed of our ATV of 5 km h^{-1}. Each logged measurement was tagged with a spatial reference coordinate using the same digital GPS receiver mentioned above. All three instruments were attached to a John Deer ATV (Fig. S3) and driven in parallel lines across the 16 ha study site, at intervals of ~3 m.

The gamma detector, or gamma-ray spectrometer (or gamma), records the amount of radioactive isotopes in the soil based on the principle that each gamma ray photon relates to a discrete energy window which is characteristic of the source isotope (Minty et al., 1998). Gamma radiometrics is a passive sensing technique the detects the varying amounts of naturally occurring radioisotopes of potassium (^{40}K), uranium (^{238}U-series) and thorium (^{232}Th-series)

Table 1
Proximal soil sensors and their characteristics.

Proximal Sensor (and nickname)	Measures	Units	Effective Depths (m)	Approximates . . .	Publications
RSX-1 Gamma Detector (Gamma)	U, K, Th, and total counts	counts per second (cps)	0.4	clay content, mineralogy, soil pH	Wilford et al. (1997), Taylor et al. (2002), McBratney et al. (2003), Pracilio et al. (2006), Wilford and Minty (2006) Stockmann et al. (2015)
DUALEM–4 s Electromagnetic Sensor (EM)	Conductivity	mS m^{-1}	0.5, 1, 1.6, 3.2	moisture content, salinity, clay content, thickness of the solum	Doolittle et al. (1994), Johnson et al. (2001), Whelan and McBratney (2003), Huth and Poulton (2007) Robertson et al. (2007), Saey et al. (2009), Zhu et al. (2010)

from soil as they produce high-energy gamma-rays with sufficient intensities to be picked up by the detector (IAEA, 2003). Additionally, a total count gamma-ray measurement was taken over the entire spectrum range. Measurements were recorded in counts per second (cps). Data from the gamma detector has been linked to many soil physical and chemical properties (Table 1). Radiometric information of the soil landscape is therefore a crucial explanatory variable of the heterogeneity of soil properties and a highly valuable asset for improving the prediction of their spatial distribution (McBratney et al., 2003). More information on the gamma radiometric analysis is provided in Table 1.

Electromagnetic induction technologies (or EM) have been used for decades to map ground conductivities in mineral exploration (Keller and Frischknecht, 1966), and more recently used to measure soil properties as applied to precision agriculture or the management of crops at a very detailed resolution (Robertson et al., 2007; Whelan and McBratney, 2003). EM sensors mostly measure bulk soil electrical conductivity (ECa). Other soil properties of interest may be inferred using EM data (e.g. soil moisture, pH and texture, Table 1). The DUALEM-21S (Dualem, Milton, ON, Canada) sensor used in this work has dual-geometry (horizontal and vertical) receivers at separations of 1- and 2-m from the transmitter. This configuration provides four simultaneous depths of conductivity sounding or depth of exploration, that correspond to integrated conductivity measurements in mS m^{-1} for depths of 0-0.5m, 0–1m, 0–1.6 m and 0–3.2 m (Table 1).

2.5. Soil physical and chemical analyses

A suite of soil chemical and physical variables was also measured, using 66 samples (0–10 cm) collected at random across the study site. These samples were collected immediately after measurements of GHG fluxes and were located within the area occupied by the dynamic chamber (5 × 5 cm). All soil samples were sieved to 2 mm. Soil inorganic nitrogen and dissolved organic C and N (DOC, DON) were extracted using 0.5 M K_2SO_4, with 5 g dry soil to 40 ml of salt solution shaken for 1 h and extracted with Whatman #1 filters. Extracts were analysed on a Lachat Quikchem 8500 (Lachat Instruments, Loveland, CO) following standard procedures for ammonium (NH_4^+) and nitrate (NO_3^-), and for DOC and DON using a Schimadzu TOC-V series analyser (Kyoto, Japan). Total C and N were analysed with a LECO CHN628 elemental analyser (LECO Corporation, St. Joseph, MI) using dried and ground soils. pH was measured with a SevenMulti probe (Mettler Toledo, Columbus, OH) using a 1:1 ratio (w:w). Concentrations of heavier elements in the soil were measured using X-ray fluorescence (XRF) with a Niton XL3 t Ultra Analyzer meter (Thermo Scientific, Waltham, MA).

2.6. Statistical analyses

Maps of gas fluxes, together with the proximally sensed gamma and EM data, were prepared at a 10 m resolution for the 16 Ha site. We used both geostatistical and digital soil mapping methods to achieve those ends (McBratney and Pringle, 1999; McBratney et al., 2003; Webster and Oliver, 2001). Local variograms and kriging were used for mapping proximal sensor data (gamma and EM). In this case, local variograms were fitted to available data within a defined spatial neighbourhood, followed by kriging. Local variogram modelling captures localized spatial features in data that may be lost, or smoothed, if a global variogram is used. Local variograms are more amenable for large data sets because they negate the need to invert large matrices. For examining the basic spatial structure of the gas flux data, we fitted whole-area (global) variogram models to measured data from both gases. Here, we considered both spherical and exponential variogram models, and selected the one that achieved highest cross-validation accuracy (i.e. smallest root mean square error, RMSE).

For mapping both gas flux variables, we wanted to exploit the availability of the mapped proximally-sensed data through the use of a regression kriging model (Odeh et al., 1995). Regression kriging is a hybridized model whereby the predictions of the target variable, in our case the gas flux data, are made via a deterministic method (regression model with covariate proximal sensor data) and a stochastic method (spatial auto-correlation of the model residuals with a variogram). The deterministic method essentially 'detrends' the data, leaving behind the residuals for which we need to investigate whether there is additional spatial structure which could be added to the regression model predictions. Subsequently in this study the predictive covariates in the regression model were the proximal sensor data. The regression model we used was quantile regression forests (QRF; Meinshausen, 2006) which is a data mining algorithm based on Random Forests (Breiman, 2001) – a boosted regression tree model. This type of non-parametric model allows flexibility in the model-fitting approach as no assumptions about the input data are required. For spatial modeling of the residuals of the QRF model we again considered either spherical or exponential variogram models. Given a variogram model, simple kriging of the residuals followed, that (if an appropriate variogram model was fitted) were added to the mapped predictions from the regression model. Prior to model fitting though, we first spit the data into two subsets. The first subset contained 70% of the available data and was designated to be used for model training; the other subset (the remaining 30%) was set aside for an independent model validation. The accuracy of the models was assessed by evaluating the RMSE and coefficient of determination (R^2) between measurements of the gas flux data from the validation data set and their corresponding regression kriging predictions.

Variogram modelling and associated kriging was performed using the VESPER software (Minasny et al., 2005). Besides QRF models which were fitted using the quantregForest R package (Meinshausen and Schiesse, 2015). All other univariate regression, descriptive statistics, and multi-variate statistics were conducted with R (R Core Team, Vienna, Austria), using the *vegan* package for multi-variate analyses (Oksanen et al., 2007).

3. Results

3.1. Temporal variability in GHG fluxes

All three GHGs showed high temporal variability, with most of activity during the early weeks of the sampling program (end of summer, beginning of autumn – February to late March). Precipitation events triggered pulses in all three gases, but in the case of CH_4 fluxes the pulses were negative (or soil consumption of atmospheric CH_4). One rain event at the end of February led to dramatic 'spiking' or surge of CO_2 and N_2O emissions (276 mg CO_2 m^{-2} h^{-1} and 34 μg N_2O m^{-2} h^{-1}), and of methane uptake (−125 μg CH_4 m^{-2} h^{-1}). We recorded strong variability in CO_2 fluxes from mid-March to April, at the end of summer.

From mid-May to mid-June (the period during which spatial variability in GHG fluxes was recorded), fluxes were smaller than earlier in the autumn (Fig. 2 and S2). Mean air temperatures for this period were less (around 12 °C), and there was less diurnal variation (Fig. S2). Mean (±SD) volumetric water content in the top 0–7 cm was 0.238 ± 0.043, and soil temperature was 16 ± 4 °C. Emissions of CO_2 were low for most of this period, except for two rain events before and after our measurements. These events created small spikes in CO_2 emissions (from ~20 mg CO_2 m^{-2} h^{-1}

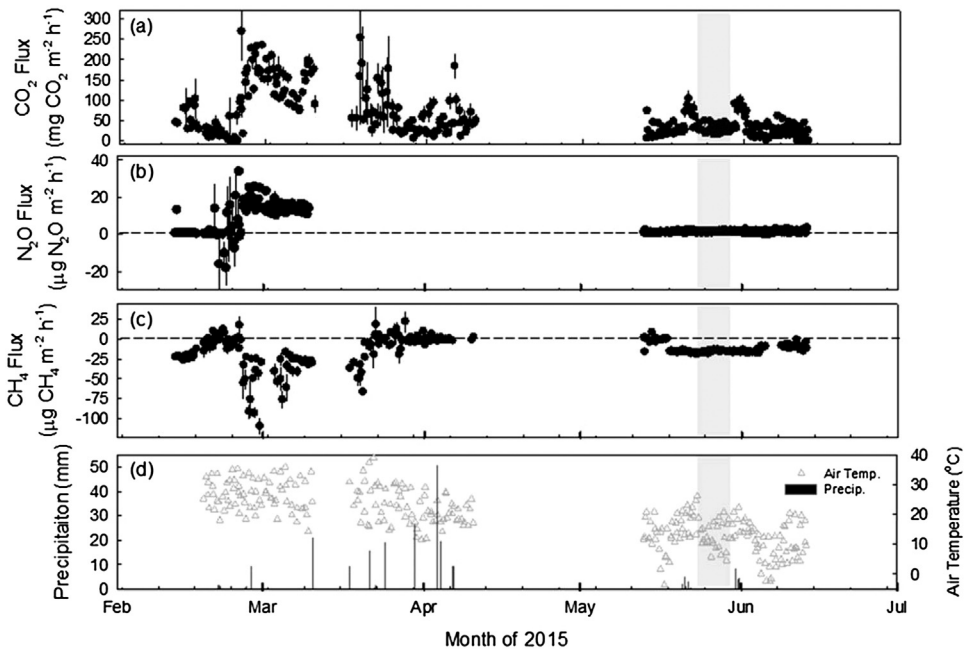

Fig. 2. Temporal variability of soil greenhouse gas fluxes. We used six automated chambers to quantify GHG emissions (a, b, and c) from February 12th to June 13th, 2015. Each data point for the GHG fluxes are a mean (n = 6) with standard error. Climate parameters were recorded simultaneously (d) with grey triangles representing 6 h mean air temperatures and filled bars precipitation. Automated chambers were located within the central 100 × 100 m, square (from Fig. 1). The spatial variability study was conducted during the period shaded in grey.

to ~ 100 mg CO_2 m^{-2} h^{-1}), but CH_4 and N_2O showed little response. All chambers recorded positive N_2O emissions during this period, and little temporal variation, resulting in a mean emission of ~1 µg N_2O m^{-2} h^{-1}. CH_4 fluxes approached 0 µg CH_4 m^{-2} h^{-1} on May 13th, and then dropped to −15 µg CH_4 m^{-2} h^{-1} on May 17th, and remained steady through the first week of June.

3.2. Spatial variability in GHG fluxes

There were clear spatial patterns in fluxes of CH_4 and N_2O between May 23rd and May 31st (Fig. 3) and very little, if any, diurnal pattern to the measurements (Fig. S4). First, CH_4 and N_2O fluxes were not well correlated between each other. Instead, each gas showed unique spatial patterns (Fig. 3). A general north-south trend in fluxes of CH_4 can be contrasted with a more east-west trend in N_2O fluxes (Fig. 3). Secondly, soils mostly emitted N_2O (82% of area) but took up CH_4 (94% of area). Fluxes of both gases, were highly variable. CH_4 fluxes had a standard deviation of 42 µg CH_4 m^{-2} h^{-1} while those of N_2O had a standard deviation of 20 µg N_2O m^{-2}. Rates of methane uptake were greatest at the northern end of study site, −327 µg CH_4 m^{-2} h^{-1}, while maximum rates of emission were 237 µg CH_4 m^{-2} h^{-1} (Table S1). N_2O emissions peaked at 476 µg N_2O m^{-2} h^{-1}, with a minimum of −19 µg N_2O m^{-2} h^{-1}. When data were mapped, 37% of the mean negative CH_4 flux could be attributed to just 1% of the area. For N_2O, 48% of the mean flux was attributable to 1% of the area.

Interpretation of semivariograms is based on the "first rule of geography" – that variables closer together are more similar than those far apart. There are three important values in a semivariogram: the nugget, sill, and range. The nugget is the y-intercept of the semivariogram, and represents the variability that cannot be explained by the distance between variables. The sill is the asymptote of the semivariogram and represents the maximum observed variability in the data. Finally, the range is the distance

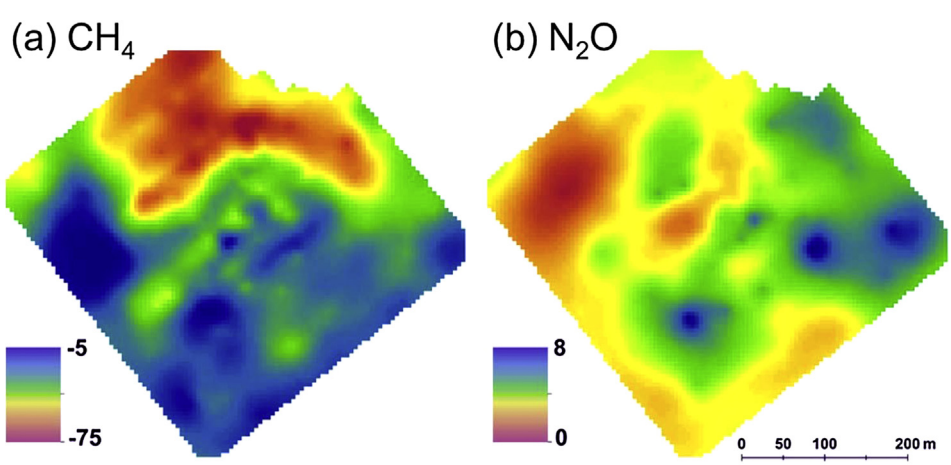

Fig. 3. Spatial variability of soil greenhouse gas fluxes at the end of May across the 16 ha site (Fig. 1). Derived maps of methane (a) and nitrous oxide (b) fluxes (µg (CH_4 or N_2O) m^{-2} h^{-1}).

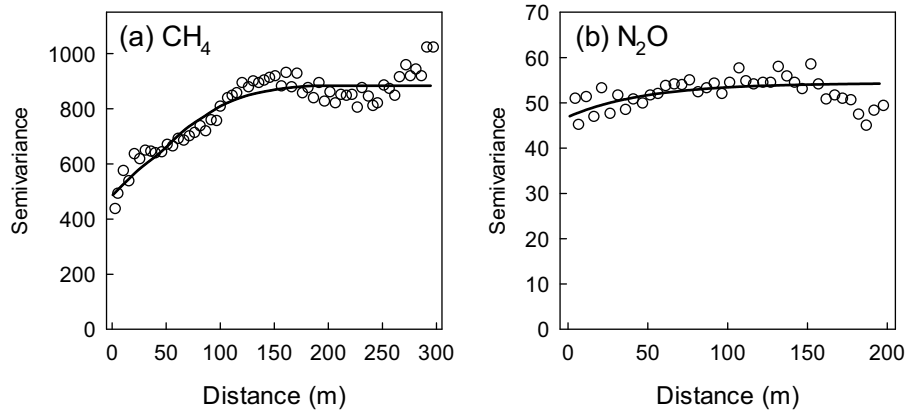

Fig. 4. Semivariograms from the spatial variability study (Fig. 2). Semivariograms for CH_4 (a) and N_2O (b) fluxes. Trend lines for both gases used the spherical variogram model.

where the semivariance no longer increases, or where the variables are independent and no longer related. Our semivariance analysis revealed that fluxes of both GHG had unique autocorrelations with distance (Fig. 4). N_2O had a nugget semivariance value of 48, a sill of 54, and a range of 112 m. CH_4, on the other hand, had a nugget value of 489, a sill of 880, and a range of 157 m. Both nugget values suggest either significant spatial variation at distances smaller than our sampling intervals (<5 m), or measurement errors. A larger sill value for CH_4 fluxes suggests greater variability compared to N_2O fluxes. The greater range for CH_4 also suggests a greater distance over which fluxes are autocorrelated, compared to that of N_2O. Nugget-to-sill ratios are generally regarded as indicators of spatial dependence – the smaller the value the greater the spatial dependency. For CH_4 the nugget-to-sill ratio was 0.55, and for N_2O it was 0.89–indicating moderate and weak spatial autocorrelation, respectively. The CH_4 semivariogram also shows some cyclicity, or oscillation in semivariance, suggesting heterogeneity in variance at greater distances (>150 m).

Regression kriging of the gas flux measurements returned mixed results. It was found that a QRF model using solely the proximal sensing data was the most appropriate for both variables. The covariate data effectively de-trended the data to the point that there was no evident spatial structure in the QRF model residuals based on nugget. Based on the validation data we estimated the RMSE between measurements and predictions to be 26 and 6 $\mu g\, m^{-2}\, h^{-1}$ for CH_4 and N_2O fluxes respectively. R^2 for both gas flux variables was 24% and 7% respectively. These results indicate that spatial prediction of CH_4 is more certain in comparison to N_2O.

We compared the spatial variability in soil GHG fluxes to both five months of temporal variation (Tables S1 and S2) and eight days during which we measured the spatial variability. Even if we focus on the inner square of 1 ha, there is enormous spatial variability of both gases during the spatial campaign, compared to that temporal

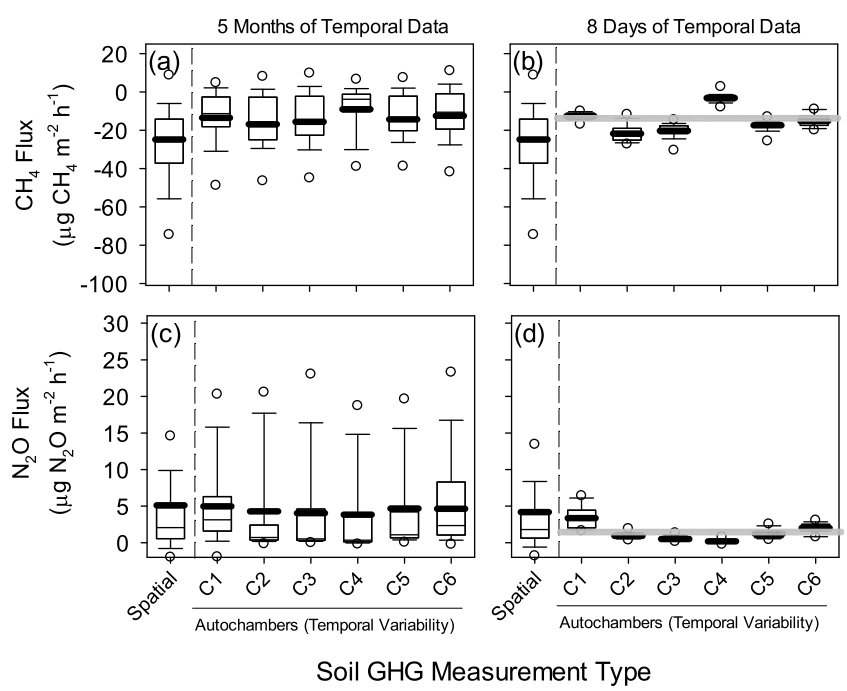

Fig. 5. Boxplots showing the spatial variability (n = 432) of soil CH_4 (a, b) and N_2O (b, d) fluxes in the 1 ha inner-square (Fig. 1) versus temporal variability of six autochambers during two periods: five months (n = 203–280) and eight days (n = 18–28). The eight days were during when the spatial GHG measurements took place. Open circles indicate the 5th and 95th percentiles, and means are the thicker bar.

Table 2
Statistical metrics and spatial variation of soil proximal sensor data.

Proximal Sensor and Variables	Descriptive Statistic								
	n	Mean	Standard Deviation	CV (%)	Min	25th Quartile	Median	75th Quartile	Max
Gamma Detector (cps)									
Uranium	1030	6.6	0.5	7.3	4.8	6.2	6.6	6.6	8.5
Thorium	1030	9.0	0.6	6.5	6.9	8.7	9.0	9.6	12.0
Potassium	1030	35.4	2.8	7.9	26.2	34.1	35.2	35.6	45.9
Total	1030	288.1	15.3	5.3	238.0	278.1	289.5	292.2	333.2
Electromagnetic Sensor ($mS\,m^{-1}$)									
0–0.5 m	1030	44	6	14.1	14	42	44	47	58
0–1 m	1030	69	12	16.9	25	67	68	76	102
0–1.6 m	1030	75	12	16.7	28	73	74	82	108
0–3.2 m	1030	89	17	19.5	42	84	86	96	139

variability of six autochambers (Fig. 5). For CH_4, the five-month the temporal mean (±SD) was -14 ± 20 CH_4 $m^{-2}\,h^{-1}$, while the spatial mean at the end of May was -31 ± 42 μg CH_4 $m^{-2}\,h^{-1}$. The temporal and spatial ranges for CH_4 were −125–54 and −327–237 μg CH_4 $m^{-2}\,h^{-1}$, respectively. The temporal mean (±SD) for N_2O was 1 ± 14 μg N_2O $m^{-2}\,h^{-1}$, by contrast the spatial was 5 ± 20 μg N_2O $m^{-2}\,h^{-1}$. The temporal and spatial ranges for N_2O were −129–63 and −19–476 N_2O $m^{-2}\,h^{-1}$, respectively.

3.3. Proximal soil sensing

Proximal sensors (Table 1) provided data on variation of soil properties at a fine spatial resolution. Gamma radiometric data showed strong signals for potassium (Table 2); and higher counts from east to west (Fig. 6). The thorium readings were more spatially fragmented. We recorded large counts at the south and east and small counts in the centre of the study site. Uranium counts were greatest at the south-eastern edge of the site. Thorium counts are commonly related to clay content of soils, since radioisotopes of thorium are preferentially scavenged by secondary clay minerals.

EM responses for the four soil depths showed a somewhat similar spatial pattern – there was little change in the spatial variation with depth (Fig. 7). There was a slight increase in coefficient of variation (CV) with depth (38%, Table 2). This becomes clearer at finer vertical resolution (see Fig. S5a). A general increase in conductivity with depth is mostly associated with soil

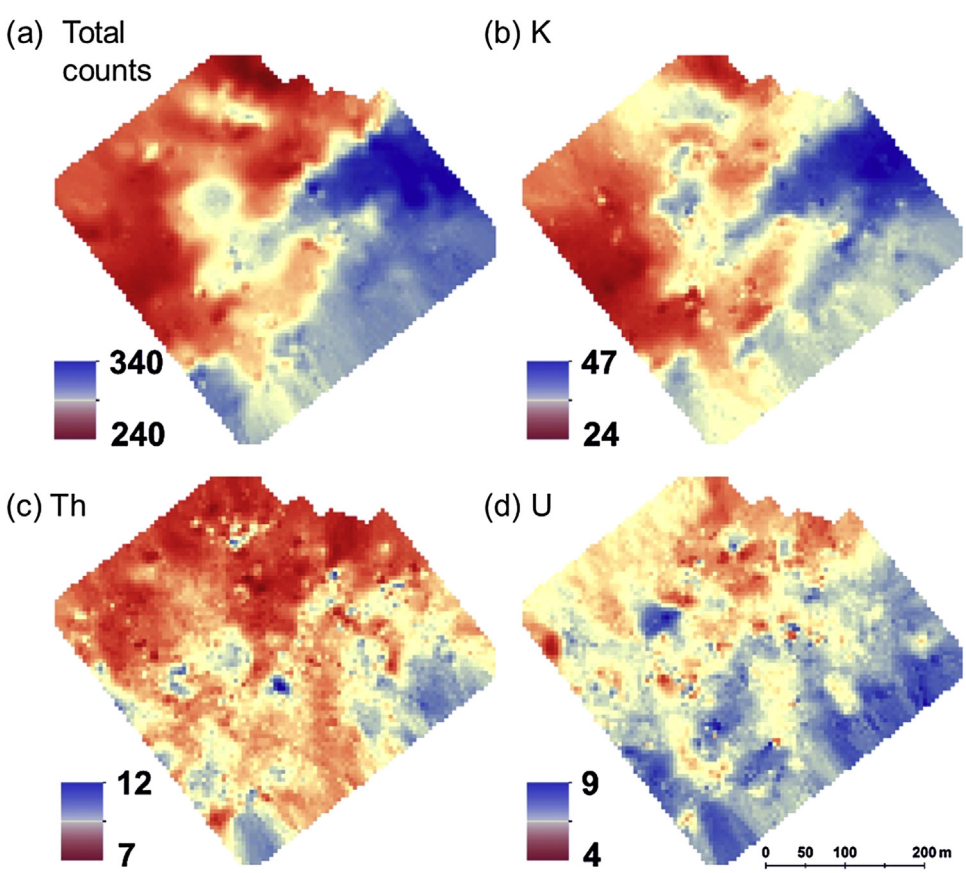

Fig. 6. Spatial variability of the radiometric data at the end of May across the 16 ha site (Fig. 1). The Gamma proximal sensor data is in counts per second (CPS) for the total counts (a), potassium (b), thorium (c), and uranium (d).

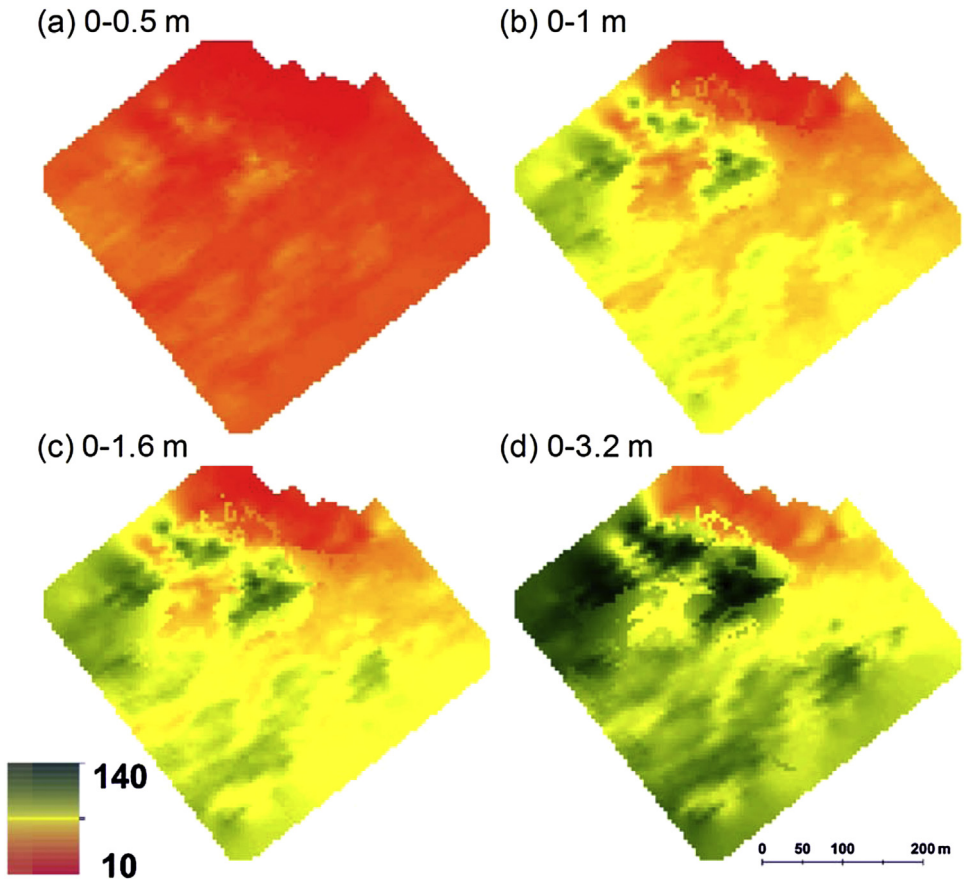

Fig. 7. Spatial variability of the conductivity data at the end of May across the 16 ha site (Fig. 1). The dual-EM conductivity data measured at 0-0.5 m (a), 0–1 m (b), 0–1.6 m (c), and 0–3.2 m (d) depths. See Fig. S5 for graphs on individual scales.

moisture. Conductivity (and likely soil moisture) at all depths was greatest in the south and west areas of the study site (Fig. 7).

Soil chemical analyses revealed greater spatial variability for known dynamic variables (e.g. ammonium, nitrate, DOC, and DON; Table 3). Some alkali earth metals (e.g. Ca, Mg), transition metals (e.g. Co), and halogens (e.g. Cl) also showed considerable spatial variability over the site. Soil C ranged from 0.9 to 2.2%, and N from 0.05 to 0.2%. Total concentrations of inorganic N ranged from < 1 to > 163 mg kg^{-1}. DOC and DON had ranges of 56–235 and 8–670 mg kg^{-1}, respectively.

Table 3
Spatial Pearson correlation coefficients (r) between nitrous oxide (N_2O) and methane (CH_4) fluxes and proximal soil sensor data.

Correlate	CH_4	N_2O
Greenhouse Gases (μg m^{-2} h^{-1})		
CH_4	1.00	−0.03
N_2O	−0.03	1.00
Gamma Detector (cps)		
Uranium	0.49	0.25
Thorium	0.52	0.28
Potassium	−0.21	0.48
Total CPS	0.10	0.51
Electromagnetic Sensor (mS m^{-1})		
0–0.5 m	0.74	−0.21
0–1 m	0.63	−0.33
0–1.6 m	0.62	−0.32
0–3.2 m	0.42	−0.43

3.4. Relationships between soil properties and greenhouse gas fluxes

Data from the two proximal sensors related differently to fluxes of CH_4 and N_2O (Table 3). Both proximal sensors related more strongly to CH_4 than to N_2O. Conductivity between 0 and 0.5 m was best related to CH_4 fluxes (r = 0.74). CH_4 was also best correlated with Thorium counts from the gamma sensor (r = 0.52). While CH_4

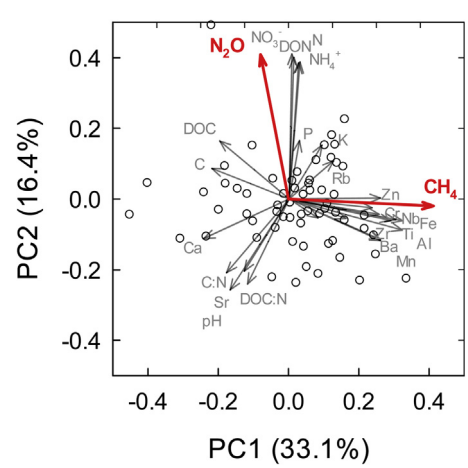

Fig. 8. Principal component analysis of the soil chemical parameters (grey) measured at the Campey site (n = 66). Soil samples are from 0 to 10 cm depth. The x- and y-axes are the principal components (PC), and explain a total of 49.5% of the variation among the sampling locations. Also shown are correlations with CH_4 and N_2O fluxes (red, *P* values less than 0.033).

and N_2O were positively correlated with most of the gamma data, CH_4 was negatively correlated with K ($r = -0.21$). N_2O fluxes, on the other hand, were negatively correlated with soil electrical conductivity (Table3), but best correlated to K counts ($r = 0.48$).

Chemical characteristics of soil samples also varied substantially (Table S3), and some individually correlated well with CH_4 and N_2O (Table S4; Figs. S6 and S7). Using a multi-variate technique (principal components analysis, PCA), 50% of the variability could be resolved using two principal components (Fig. 8). Fluxes of both GHGs were positively correlated with chemical variables (*P* values: N_2O 0.017, CH_4 0.033) and each gas was orthogonal and associated with a different PC. There were many expected correlations within soil chemical properties – for instance inorganic N is correlated with total N (and DOC with total C). CH_4 fluxes were better represented with PC1 and correlated best with Zn, Al, and Fe concentrations, and negatively with total C and DOC (Fig. 8). N_2O fluxes were best reflected in variables along PC2 – positively associated with inorganic N, DON, and total N, but also P and gamma-K, and negatively correlated with pH.

4. Discussion

4.1. On the spatiotemporal variability of soil CH_4 and N_2O fluxes

Spatiotemporal variability, and our capacity to measure it, is a major obstacle to prediction and mitigation of GHG emissions from soils. Particularly strong spatiotemporal variability in fluxes of CH_4 and N_2O make it exceedingly difficult to make recommendations to reduce fluxes (Hénault et al., 2012; Paustian et al., 2016). The data presented here are a first attempt to simultaneously measure both the spatial and temporal variability of CH_4 and N_2O at a reasonable scale (16 ha), within a field that has relatively homogeneous soils. At our study site, there has been little variability in vegetation for many decades, and the general landscape of the entire region is very flat – most < 1.8% slope. Even 1 m deep soil cores from these grey cracking clay soils show little horizon differences (Fig. S8). Other studies have found strong variability in CH_4 and N_2O fluxes associated with variation in topography (Bellingrath-Kimura et al., 2014; Imer et al., 2013; Konda et al., 2010; Lark et al., 2004), different vegetation communities (Sturtevant and Oechel, 2013; Lai et al., 2014), or across ecosystem transitions (i.e. ecotones, Hefting et al., 2006; Jacinthe et al., 2015). Such variation is not surprising given the influence of these soil forming factors on soil properties (Brubaker et al., 1993; Kieft et al., 1998) – especially on soil biological parameters (Cambardella et al., 1994; Florinsky et al., 2004; Wickings et al., 2016). In our case, however, the landscape has little relief and major soil forming factors such as climate, time, and plant species were more or less uniform across the site. Clearly, other subtler influences are at play.

The spatial CV was just 8% less than the temporal CV (~5 months) for CH_4, while for N_2O the same comparison was 68% (Fig. 3 and Tables S1 & S2). Coefficients of variation are less informative when values range from positive to negative (as in our GHG fluxes), and especially if mean values approach zero (Webster, 2001). For our data it is perhaps more helpful to consider comparisons of raw standard deviations (SD). In our case the spatial SD was 112% and 39% greater than temporal SD for CH_4 (Table S1) and N_2O (Table S2), respectively. Semivariance analysis of the two gases showed high nugget values (Fig. 4), indicating that a significant amount of variability in CH_4 and N_2O is likely found at even smaller distances than we measured here (i.e. <5 m).

A key issue in determining landscape-scale fluxes are the contributions of different parts of the landscape to the overall flux. "Hot spots" (Cowan et al., 2015; Groffman et al., 2009; McClain et al., 2003) for emissions have long been noted and contribute to the general lack of uniformity of fluxes. For example, a survey of N_2O fluxes from a pasture showed that an area of 1.1% contributed > 55% of the N_2O fluxes from 7 ha of pasture (Cowan et al., 2015). In our study we found hot spots for both greenhouse gas emissions. For example, only 5% of our study area had positive CH_4 fluxes, and the mean flux of this area was 44 $\mu g\ CH_4\ m^{-2}\ h^{-1}$. For N_2O, 24% of positive emissions came from just 1% of the area.

It is also worth noting that our spatial variability measurements were collected over a short period with low overall CH_4 and N_2O fluxes (Fig. 2 and S2). Some studies have shown that periods of greater fluxes show more spatial variability (Bellingrath-Kimura et al., 2014; Konda et al., 2010). It is possible that large rainfall events or high summer temperatures (e.g. end of February in our study, Fig. 2) could further increase the spatial variability at our study site. High-frequency flux measurements, as described here, can now be used to test the hypothesis that "hot moments drive hot spots." The frequent use of eddy flux and eddy gradient methods to measure soil GHG emissions from the fields has worked well for capturing temporal variability (Wang et al., 2013; Peltola et al., 2015), but our work clearly shows we may be missing large within-field variability that is crucial for management decisions since management also occur at this scale.

If we used the 8-day, six-autochamber mean during our spatial measurement period (Figs. S2), we would underestimate fluxes in our inner square (1 ha) by 59 and 197%, for CH_4 oxidation and N_2O efflux respectively (Fig. 5). There are two important methodological issues to consider. First, the small chamber size, and disturbance from inserting the chamber, may have led to overestimation of our flux measurements (Hutchinson and Livingston, 2002). Second, our spatial measurements also occurred through time (over 8 days in May), thus spatial variability was not completely isolated from temporal dynamics. These were trade-offs we were willing to accept due to the logistical difficulty of doing a spatial GHG flux study at this scale with pre-inserted gas flux collars. However, our data do not support an overwhelming disturbance effect, nor a strong temporal interference, from our spatial gas flux method. Out of our 432 spatial measurements in the inner 1 ha square (Fig. 1), a large number of measurements were less than the temporal N_2O mean (41%), or the CH_4 oxidation mean (27%), over the 8 days from the fixed-collar autochambers (Fig. 5). Because nearly over a third of both of our GHG flux measurements were less than the mean from these collared chambers, it is more likely that the difference in fluxes between the spatial and temporal measurements were the result of spatial variability, rather than consistent overestimation from chamber disturbance. Finally, even though the spatial measurements took place over time we showed very little temporal variability in the autochambers during this measurement period (Figs. S2 & S4). Other researchers have measured spatial variability of soil GHGs within a range of 1–17 days (Velthof et al., 1996; Konda et al., 2010; Giltrap et al., 2014; Cowan et al., 2015) and found diurnal variability to be small with respect to spatial variability. It is evident that in this agricultural field, during a low GHG flux period (i.e. winter), there was enormous spatial variability not represented by our autochambers.

Adequate sampling frequency, in both time and space, is a major logistic hurdle for GHG studies. Velthof et al. (1996) attempted to define an adequate sampling density and found that 375–1240 samples were needed to reduce variability such that the sample mean was within 10% of the true mean. Such sampling frequencies have seldom been attempted. Some studies have suggested that fluxes can be reliably estimated by a modest number of larger chambers (Weitz et al., 1999). Weitz et al. (1999) found that spatial variability of N_2O fluxes within a plot 1/10 the size of our study area (0.16 ha) were adequately estimated by 8 chambers (total measurement area of 0.46 m^2). In our study site of 16 ha, the number of samples (e.g. 0.023 m^2 chambers) required to reduce

sample variance such that sample means were within 10% of 'true' means was 1910 for CH_4 and 8248 for N_2O. In many, if not all situations, methodical analysis of spatial variability is an essential pre-condition for scaling of soil GHG fluxes from manual or even automated chambers to large fields, or beyond to regional or even national scales.

4.2. Relationships between soil properties and greenhouse gas fluxes

Inconsistent relationships of both CH_4 and N_2O to soil temperature and moisture indicate a complex interplay among responsible microbial populations, their substrates used for producing (or consuming) GHGs, and other soil factors. Because most studies of the fluxes of these two GHGs focus on variability over time, influences of temperature and moisture can obscure more nuanced and subtle influences of soil properties. We explored how spatial variation in soil physical and chemical properties might explain the spatial variability of soil CH_4 and N_2O fluxes, within relatively constant conditions of soil temperature and moisture.

CH_4 fluxes are known to have a strong spatial dependence relative to those of N_2O (Bellingrath-Kimura et al., 2014; Konda et al., 2010; van den Pol-van Dasselaar et al., 1998), as confirmed here (Fig. 4). We found strong relationships between CH_4 and proximal soil sensors (Table 3). A measure of soil electrical conductivity (as influenced by soil moisture) provided the best predictive ability for CH_4 (Figs. 3, 7, and S5). Other studies have shown that while high fluxes of CH_4 uptake are generally related to periods of low soil moisture content (Boeckx and Van Cleemput, 1996; Born et al., 1990; Hiltbrunner et al., 2012; Keller and Reiners, 1994), moisture alone is often only weakly predictive of CH_4 fluxes (Tang et al., 2006; Konda et al., 2010; Sullivan et al., 2010). While our proximal sensing data did not provide a strong basis for predicting N_2O fluxes, the total gamma counts (Table 3) suggested that soil texture, pH, and/or mineralogy play roles in spatial variability.

A suite of soil chemical characteristics explained nearly 50% of spatial variation in both GHG fluxes. Not surprisingly, N_2O fluxes were best related to forms of nitrogen (total, inorganic, and dissolved organic forms; Fig. 8), but also to DOC. Previous research has linked N_2O fluxes to available reactive N (Butterbach-Bahl et al., 2013; Shcherbak et al., 2014; Weier et al., 1993) and DOC (Bayer et al., 2015; Morley and Baggs, 2010). Less understood are roles of other nutrients, like phosphorus, in limiting N_2O production (Baral et al., 2014; Mori et al., 2010); as also shown here (Fig. 8). We can speculate, based on abundance as measured by XRF and by the gamma detector in our proximal sensors, that K availability might also influence N_2O emissions (see Figs. 3 and 6).

CH_4 fluxes were negatively related to both total C and DOC. Some recent studies suggest that soil CH_4 uptake may be linked to very labile forms of C (Pratscher et al., 2011; Sullivan et al., 2013), but we lack a mechanistic link to methanotrophic activity. Notionally, greater concentrations of DOC and total C are reflected in greater microbial biomass and general microbial activity. CH_4 fluxes were positively correlated to the abundances of several metals including Fe, Al, and Zn (Fig. 8). Cu and Zn are cofactors for the particulate methane monooxygenase enzyme used by methanotrophs to oxidize CH_4 (Lieberman and Rosenzweig, 2005). Zn varied more in our soils than Cu, and showed a stronger positive relationship with CH_4 uptake indicating its availability might play a role.

5. Conclusions

Spatial variability is a pernicious problem in soil GHG research. Many studies are limited to as few as three (but typically no more than five) small chambers and then assume that this sampling density is adequate to represent areas of hundreds, or even thousands of hectares. Our research and that of others shows this assumption to be poorly based (Cowan et al., 2015; Imer et al., 2013; Kravchenko and Robertson, 2015). Measuring and understanding the causes of spatial variability in soil GHG fluxes is central to improving the robustness of flux estimates for all ecosystems in general, but specifically for agroecosystems. Our second objective was to test if proximal sensors could be used to improve our ability to cope with spatial variability. The answer is a conditional yes. With further development, proximal sensors combined with modelling may help resolve issues around spatial variability. Likely improvements in sensor technology will quickly improve our ability to quantify spatial variability in factors (e.g. reactive N) known to be limiting to or supportive of the microbial activity responsible for fluxes of CH_4 and N_2O. At the very least, proximal sensors can help quickly identify how best to deploy GHG flux sampling and predict locations of "hotspots" of emissions. Targeting these 'troublesome' areas with management interventions (i.e. precision agriculture) designed to reduce emissions will be part of overall emission reduction strategies (Paustian et al., 2016). This is especially important for countries like Australia, where the agriculture sector is a large portion (23%) of the total national GHG emissions (Hatfield-Dodds et al., 2007; Maraseni and Cockfield, 2011).

Acknowledgements

We would like to thank DAFF Carbon Farming Futures, Action on the Ground project, ARC Linkage LP120200521 for funding for this project. Much appreciation and thanks to Richard Heath and Peter Bell at the University of Sydney Plant Breeding Institute in Narrabri, NSW for field operations help and logistical support. We would like to extend a special thanks to Carmello Maucieri, Yaojun Zhang, and Hero Tahaei for field and/or laboratory assistance. Lastly, we would like to thank Bradley Miller for providing feedback on a draft of this manuscript.

Appendix A. Supplementary data

Supplementary data associated with this article can be found, in the online version, at http://dx.doi.org/10.1016/j.agee.2017.02.017.

References

Baral, B.R., Kuyper, T.W., Van Groenigen, J.W., 2014. Liebig's law of the minimum applied to a greenhouse gas: alleviation of P-limitation reduces soil N_2O emission. Plant Soil 374, 539–548.

Bayer, C., Gomes, J., Zanatta, J.A., Vieira, F.C.B., Piccolo, M., de, C., Dieckow, J., Six, J., 2015. Soil nitrous oxide emissions as affected by long-term tillage, cropping systems and nitrogen fertilization in Southern Brazil. Soil Tillage Res. 146, 213–222. doi:http://dx.doi.org/10.1016/j.still.2014.10.011.

Bellingrath-Kimura, S.D., Kishimoto-Mo, A.W., Oura, N., Sekikawa, S., Yonemura, S., Sudo, S., Hayakawa, A., Minamikawa, K., Takata, Y., Hara, H., 2014. Differences in the spatial variability among CO_2, CH_4, and N_2O gas fluxes from an urban forest soil in Japan. Ambio 44, 55–66. doi:http://dx.doi.org/10.1007/s13280-014-0521-z.

Boeckx, P., Van Cleemput, O., 1996. Methane oxidation in a neutral landfill cover soil: influence of moisture content, temperature, and nitrogen-turnover. J. Environ. Qual. 25, 178–183. doi:http://dx.doi.org/10.2134/jeq1996.00472425002500010023x.

Born, M., Dörr, H., Levin, I., 1990. Methane consumption in aerated soils of the temperate zone. Tellus B 42, 2–8.

Breiman, L., 2001. Random forests. Machine Learning 41, 5–32.

Brubaker, S.C., Jones, A.J., Lewis, D.T., Frank, K., 1993. Soil properties associated with landscape position. Soil Sci. Soc. Am. J. 57, 235–239. doi:http://dx.doi.org/10.2136/sssaj1993.03615995005700010041x.

Butterbach-Bahl, K., Gasche, R., Breuer, L., Papen, H., 1997. Fluxes of NO and N_2O from temperate forest soils: impact of forest type, N deposition and of liming on the NO and N_2O emissions. Nutr. Cycl. Agroecosyst. 48, 79–90. doi:http://dx.doi.org/10.1023/A:1009785521107.

Butterbach-Bahl, K., Baggs, E.M., Dannenmann, M., Kiese, R., Zechmeister-Boltenstern, S., 2013. Nitrous oxide emissions from soils: how well do we understand the processes and their controls? Philos. Trans. R. Soc. London B Biol. Sci. 368, 20130122.

Cambardella, C.A., Moorman, T.B., Parkin, T.B., Karlen, D.L., Novak, J.M., Turco, R.F., Konopka, A.E., 1994. Field-scale variability of soil properties in central Iowa soils. Soil Sci. Soc. Am. J. 58, 1501–1511. doi:http://dx.doi.org/10.2136/sssaj1994.03615995005800050033x.

Cavigelli, M.A., Lengnick, L.L., Buyer, J.S., Fravel, D., Handoo, Z., McCarty, G., Millner, P., Sikora, L., Wright, S., Vinyard, B., 2005. Landscape level variation in soil resources and microbial properties in a no-till corn field. Appl. Soil Ecol. 29, 99–123.

Cowan, N.J., Famulari, D., Levy, P.E., Anderson, M., Bell, M.J., Rees, R.M., Reay, D.S., Skiba, U.M., 2014. An improved method for measuring soil N_2O fluxes using a quantum cascade laser with a dynamic chamber. Eur. J. Soil Sci. 65, 643–652.

Cowan, N.J., Norman, P., Famulari, D., Levy, P.E., Reay, D.S., Skiba, U.M., 2015. Spatial variability and hotspots of soil N2O fluxes from intensively grazed grassland. Biogeosciences 12, 1585–1596.

Doolittle, J.A., Sudduth, K.A., Kitchen, N.R., Indorante, S.J., 1994. Estimating depths to claypans using electromagnetic induction methods. J. Soil Water Cons. 49, 572–575.

Florinsky, I.V., McMahon, S., Burton, D.L., 2004. Topographic control of soil microbial activity: a case study of denitrifiers. Geoderma 119, 33–53.

Giltrap, D.L., Berben, P., Palmada, T., Saggar, S., 2014. Understanding and analysing spatial variability of nitrous oxide emissions from a grazed pasture. Agr. Ecosyst. Environ. 186, 1–10.

Gregorich, E.G., Rochette, P., VandenBygaart, A.J., Angers, D.A., 2005. Greenhouse gas contributions of agricultural soils and potential mitigation practices in Eastern Canada. Soil Tillage Res. 83, 53–72.

Griffith, D.W.T., Galle, B., 2000. Flux measurements of NH_3, N_2O and CO_2 using dual beam FTIR spectroscopy and the flux–gradient technique. Atmos. Environ . 34, 1087–1098. doi:http://dx.doi.org/10.1016/S1352-2310(99)00368-4.

Groffman, P., Butterbach-Bahl, K., Fulweiler, R., Gold, A., Morse, J., Stander, E., Tague, C., Tonitto, C., Vidon, P., 2009. Challenges to incorporating spatially and temporally explicit phenomena (hotspots and hot moments) in denitrification models. Biogeochemistry 93, 49–77. doi:http://dx.doi.org/10.1007/s10533-008-9277-5.

Hénault, C., Grossel, A., Mary, B., Roussel, M., Léonard, J., 2012. Nitrous oxide emission by agricultural soils: a review of spatial and temporal variability for mitigation. Pedosphere 22, 426–433.

Hatfield-Dodds, S., Carwardine, J., Dunlop, M., Graham, P., Klein, C., 2007. Rural Australia providing climate solutions. Preliminary Report to the Austrailian Agricultural Alliance on Climate Change. CSIRO Sustainable Ecosystems, Canberra, ACT.

Hefting, M.M., Bobbink, R., Janssens, M.P., 2006. Spatial variation in denitrification and N_2O emission in relation to nitrate removal efficiency in a N-stressed riparian buffer zone. Ecosystems 9, 550–563.

Hensen, A., Groot, T.T., Van den Bulk, W.C.M., Vermeulen, A.T., Olesen, J.E., Schelde, K., 2006. Dairy farm CH_4 and N_2O emissions, from one square metre to the full farm scale. Agr. Ecosyst. Environ. 112, 146–152.

Hiltbrunner, D., Zimmermann, S., Karbin, S., Hagedorn, F., Niklaus, P.A., 2012. Increasing soil methane sink along a 120-year afforestation chronosequence is driven by soil moisture. Glob. Chang. Biol. 18, 3664–3671. doi:http://dx.doi.org/10.1111/j.1365-2486.2012.02798.x.

Hutchinson, G.L., Livingston, G.P., 2002. Soil-atmosphere gas exchange. In: Dane, J. H., Topp, G.C. (Eds.), Methods of Soil Analysis. Part 4. SSSA Book Ser 5 SSSA, , pp. 1159–1182 (Madison, WI).

Huth, N.I., Poulton, P.L., 2007. An electromagnetic induction method for monitoring variation in soil moisture in agroforestry systems. Soil Res. 45, 63–72.

IAEA, 2003. Guidelines for radioelement mapping using gamma ray spectrometry data. Iaea-tecdoc-1363. International Atomic Energy Agency.

Imer, D., Merbold, L., Eugster, W., Buchmann, N., 2013. Temporal and spatial variations of soil CO_2, CH_4 and N_2O fluxes at three differently managed grasslands. Biogeosciences 10, 5931–5945.

Jacinthe, P.A., Vidon, P., Fisher, K., Liu, X., Baker, M.E., 2015. Soil methane and carbon dioxide fluxes from cropland and riparian buffers in different hydrogeomorphic settings. J. Environ. Qual. 44, 1080–1090. doi:http://dx.doi.org/10.2134/jeq2015.01.0014.

Jassal, R.S., Webster, C., Black, T.A., Hawthorne, I., Johnson, M.S., 2016. Simultaneous measurements of soil CO_2 and CH_4 fluxes using laser absorption spectroscopy. Agr. Envir. Lett. 1, 1.

Johnson, C.K., Doran, J.W., Duke, H.R., Wienhold, B.J., Eskridge, K.M., Shanahan, J.F., 2001. Field-scale electrical conductivity mapping for delineating soil condition. Soil Sci. Soc. Am. J. 65, 1829–1837.

Johnson, J.M.-F., Franzluebbers, A.J., Weyers, S.L., Reicosky, D.C., 2007. Agricultural opportunities to mitigate greenhouse gas emissions. Environ. Pollut. 150, 107–124. doi:http://dx.doi.org/10.1016/j.envpol.2007.06.030.

Keller, G.V., Frischknecht, F.C., 1966. Electrical Methods in Geophysical Prospecting. Pergamon Press, New York City, NY.

Keller, M., Reiners, W.A., 1994. Soil-atmosphere exchange of nitrous oxide, nitric oxide, and methane under secondary succession of pasture to forest in the Atlantic lowlands of Costa Rica. Global Biogeochem. Cycles 8, 399–409.

Kessavalou, A., Doran, J.W., Mosier, A.R., Drijber, R.A., 1998. Greenhouse gas fluxes following tillage and wetting in a wheat-fallow cropping system. J. Environ. Qual. 27, 1105–1116. doi:http://dx.doi.org/10.2134/jeq1998.00472425002700050016x.

Kieft, T.L., White, C.S., Loftin, S.R., Aguilar, R., Craig, J.A., Skaar, D.A., 1998. Temporal dynamics in soil carbon and nitrogen resources at a grassland-shrubland ecotone. Ecology 79, 671–683 10.1890/0012-9658(1998)079[0671:TDISCA]2.0.CO;2.

Konda, R., Ohta, S., Ishizuka, S., Heriyanto, J., Wicaksono, A., 2010. Seasonal changes in the spatial structures of N_2O, CO_2, and CH_4 fluxes from Acacia mangium plantation soils in Indonesia. Soil Biol. Biochem. 42, 1512–1522.

Kravchenko, A.N., Robertson, G.P., 2015. Statistical challenges in analyses of chamber-based soil CO_2 and N_2O emissions data. Soil Sci. Soc. Am. J. 79, 200–211.

Lai, D.Y.F., Roulet, N.T., Humphreys, E.R., Moore, T.R., Dalva, M., 2012. The effect of atmospheric turbulence and chamber deployment period on autochamber CO2 and CH4 flux measurments in an ombrotrophic peatland. Biogoesci 9, 3305–3322. doi:http://dx.doi.org/10.5194/bg-9-3305-2012.

Lai, D.Y.F., Moore, T.R., Roulet, N.T., 2014. Spatial and temporal variations of methane flux measured by autochambers in a temperate ombrotrophic peatland. J. Geophys. Res.-Biogeosci. 119, 864–880. doi:http://dx.doi.org/10.1002/2013JG002410.

Lark, R.M., Milne, A.E., Addiscott, T.M., Goulding, K.W.T., Webster, C.P., O'Flaherty, S., 2004. Scale- and location-dependent correlation of nitrous oxide emissions with soil properties: an analysis using wavelets. Eur. J. Soil Sci. 55, 611–627. doi:http://dx.doi.org/10.1111/j.1365-2389.2004.00620.x.

Lessard, R., Rochette, P., Topp, E., Pattey, E., Desjardins, R.L., Beaumont, G., 1994. Methane and carbon dioxide fluxes from poorly drained adjacent cultivated and forest sites. Can. J. Soil Sci. 74, 139–146. doi:http://dx.doi.org/10.4141/cjss94-021.

Lieberman, R.L., Rosenzweig, A.C., 2005. Crystal structure of a membrane-bound metalloenzyme that catalyses the biological oxidation of methane. Nature 434, 177–182.

Longchamps, L., Khosla, R., Reich, R., Gui, D.W., 2015. Spatial and temporal variability of soil water content in leveled fields. Soil Sci. Soc. Am. J. 79, 1446–1454. doi:http://dx.doi.org/10.2136/sssaj2015.03.0098.

Mallarino, A.P., 1996. Spatial variability patterns of phosphorus and potassium in no-tilled soils for two sampling scales. Soil Sci. Soc. Am. J. 60, 1473–1481.

Maraseni, T.N., Cockfield, G., 2011. Does the adoption of zero tillage reduce greenhouse gas emissions?: An assessment for the grains industry in Australia. Agric. Syst. 104, 451–458.

McBratney, A.B., Pringle, M.J., 1999. Estimating average and proportional variograms of soil properties and their potential use in precision agriculture. Precis. Agric. 1, 125–152.

McBratney, A.B., Santos, M.L.M., Minasny, B., 2003. On digital soil mapping. Geoderma 117, 3–52.

McClain, M.E., Boyer, E.W., Dent, C.L., Gergel, S.E., Grimm, N.B., Groffman, P.M., Hart, S.C., Harvey, J.W., Johnston, C.A., Mayorga, E., McDowell, W.H., Pinay, G., 2003. Biogeochemical hot spots and hot moments at the interface of terrestrial and aquatic ecosystems. Ecosystems 6, 301–312. doi:http://dx.doi.org/10.1007/s10021-003-0161-9.

McDaniel, M.D., Kaye, J.P., Kaye, M.W., 2014. Do hot moments become hotter under climate change? Soil nitrogen dynamics from a climate manipulation experiment in a post-harvest forest. Biogeochemistry 121, 339–354. doi:http://dx.doi.org/10.1007/s10533-014-0001-3.

Minty, B.R.S., McFadden, P., Kennett, B.L.N., 1998. Multichannel processing for airborne gamma-ray spectrometry. Geophysics 63, 1971–1985.

Meinshausen, N., Schiesse, L., 2015. QuantregForest: Quantile Regression Forests R Package Version 1.1. . https://CRAN.R-project.org/package=quantregForest.

Meinshausen, N., 2006. Quantile regression forests. J. Mach. Learn. Res. 7, 983–999.

Miller, B.A., Koszinski, S., Hierold, W., Rogasik, H., Schröder, B., Van Oost, K., Wehrhan, M., Sommer, M., 2016. Towards mapping soil carbon landscapes: issues of sampling scale and transferability. Soil Tillage Res. 156, 194–208.

Minasny, B., McBratney, A.B., Whelan, B.M., 2005. VESPER Version 1.62. Australian Centre for Precision Agriculture, McMillan Building A05, The University of Sydney, NSW.

Mori, T., Ohta, S., Ishizuka, S., Konda, R., Wickaksono, A., Heriyanto, J., Hardjono, A., 2010. Effects of phosphorus addition on N_2O and NO emissions from soils of an Acacia mangium plantation. Soil Sci. Plant Nutr. 56, 782–788. doi:http://dx.doi.org/10.1111/j.1747-0765.2010.00501.x.

Morley, N., Baggs, E.M., 2010. Carbon and oxygen controls on N_2O and N_2 production during nitrate reduction. Soil Biol. Biochem 42, 1864–1871. doi:http://dx.doi.org/10.1016/j.soilbio.2010.07.008.

Odeh, I.O.A., McBratney, A.B., Chittleborough, D.J., 1995. Further results on prediction of soil properties from terrain attributes- heterotopic co-kriging and regression kriging. Geoderma 67 (3-4), 215–226.

Oksanen, J., Blanchet, F.G., Kindt, R., Legendre, P., Minchin, P.R., O'Hara, R.B., Simpson, G.L., Solymos, P., Stevens, M.H.H., Wagner, H., 2007. Vegan: Community Ecology Package. , pp. 10.

Paustian, K., Lehmann, J., Ogle, S., Reay, D., Robertson, G.P., Smith, P., 2016. Climate-smart soils. Nature 532, 49–57.

Peltola, O., Hensen, A., Marchesini, L.B., Helfter, C., Bosveld, F.C., van den Bulk, W.C. M., Haapanala, S., van Huissteden, J., Laurila, T., Lindroth, A., Nemitz, E., Rockmann, T., Vermeulen, A.T., Mammarella, I., 2015. Studying the spatial variability of methane flux with five eddy covariance towers of varying height. Agric. For. Meteorol. 214, 456–472.

Pracilio, G., Adams, M.L., Smettem, K.R.J., Harper, R.J., 2006. Determination of spatial distribution patterns of clay and plant available potassium contents in surface soils at the farm scale using high resolution gamma ray spectrometry. Plant Soil 282, 67–82.

Pratscher, J., Dumont, M.G., Conrad, R., 2011. Assimilation of acetate by the putative atmospheric methane oxidizers belonging to the USCα clade. Environ. Microbiol. 13, 2692–2701. doi:http://dx.doi.org/10.1111/j.1462-2920.2011.02537.x.

Pumpanen, J., Ilvesniemi, H., Peramaki, M., Hari, P., 2003. Seasonal patterns of soil CO_2 efflux and soil air CO_2 concentration in a Scots pine forest: comparison of two chamber techniques. Glob. Chang. Biol. 9, 371–382. doi:http://dx.doi.org/10.1046/j.1365-2486.2003.00588.x.
Robertson, M., Isbister, B., Maling, I., Oliver, Y., Wong, M., Adams, M., Bowden, B., Tozer, P., 2007. Opportunities and constraints for managing within-field spatial variability in Western Australian grain production. Field Crop Res. 104, 60–67. doi:http://dx.doi.org/10.1016/j.fcr.2006.12.013.
Saey, T., Van Meirvenne, M., Vermeersch, H., Ameloot, N., Cockx, L., 2009. pedotransfer function to evaluate the soil profile textural heterogeneity using proximally sensed apparent electrical conductivity. Geoderma 150, 389–395.
Savage, K., Phillips, R., Davidson, E., 2014. High temporal frequency measurements of greenhouse gas emissions from soils. Biogeosciences 11, 2709–2720.
Shcherbak, I., Millar, N., Robertson, G.P., 2014. Global metaanalysis of the nonlinear response of soil nitrous oxide (N_2O) emissions to fertilizer nitrogen. Proc. Natl. Acad. Sci. 111, 9199–9204. doi:http://dx.doi.org/10.1073/pnas.1322434111.
Stockmann, U., Malone, B.P., McBratney, A.B., Minasny, B., 2015. Landscape-scale exploratory radiometric mapping using proximal soil sensing. Geoderma 239, 115–129.
Sturtevant, C.S., Oechel, W.C., 2013. Spatial variation in landscape-level CO2 and CH4 fluxes from arctic coastal tundra: influence from vegetation wetness, and the thaw lake cycle. Glob. Chang. Biol. 19, 2853–2866.
Sullivan, B.W., Kolb, T.E., Hart, S.C., Kaye, J.P., Hungate, B.A., Dore, S., Montes-Helu, M., 2010. Wildfire reduces carbon dioxide efflux and increases methane uptake in ponderosa pine forest soils of the southwestern USA. Biogeochemistry 104, 251–265. doi:http://dx.doi.org/10.1007/s10533-010-9499-1.
Sullivan, B.W., Selmants, P.C., Hart, S.C., 2013. Does dissolved organic carbon regulate biological methane oxidation in semiarid soils? Glob. Chang. Biol. 19, 2149–2157. doi:http://dx.doi.org/10.1111/gcb.12201.
Tang, X., Liu, S., Zhou, G., Zhang, D., Zhou, C., 2006. Soil-atmospheric exchange of CO_2, CH_4, and N_2O in three subtropical forest ecosystems in southern China. Glob. Chang. Biol. 12, 546–560. doi:http://dx.doi.org/10.1111/j.1365-2486.2006.01109.x.
Taylor, M.J., Smettem, K., Pracilio, G., Verboom, W., 2002. Relationships between soil properties and high-resolution radiometrics, central eastern Wheatbelt, Western Australia. Expl. Geophys. 33, 95–102.
van den Pol-van Dasselaar, A., Corré, W.J., Priemé, A., Klemedtsson, Å.K., Weslien, P., Klemedtsson, L., Stein, A., Oenema, O., 1998. Spatial variability of methane, nitrous oxide, and carbon dioxide emissions from drained grasslands. Soil Sci. Am. J. 63, 810–817.
Velthof, G.L., Jarvis, S.C., Stein, A., Allen, A.G., Oenema, O., 1996. Spatial variability of nitrous oxide fluxes in mown and grazed grasslands on a poorly drained clay soil. Soil Biol. Biochem. 28, 1215–1225.
Venterea, R.T., Spokas, K.A., Baker, J.M., 2009. Accuracy and precision analysis of chamber-based nitrous oxide gas flux estimates. Soil Sci. Soc. Am. J. 73, 1087–1093.
Wang, W., Dalal, R.A.M.C., Reeves, S.H., Butterbach-Bahl, K., Kiese, R., 2011. Greenhouse gas fluxes from an Australian subtropical cropland under long-term contrasting management regimes. Glob. Chang. Biol. 17, 3089–3101. doi:http://dx.doi.org/10.1111/j.1365-2486.2011.02458.x.
Wang, K., Zheng, X.H., Pihlatie, M., Vesala, T., Liu, C.Y., Haapanala, S., Mammarella, I., Rannik, U., Liu, H.Z., 2013. Comparison between static chamber and tunable diode laser-based eddy covariance techniques for measuring nitrous oxide fluxes from a cotton field. Agric. For. Meteorol. 171, 9–19.
Webster, R., Oliver, M.A., 2001. Geostatistics for Environmental Scientists (Statistics in Practice). John Wiley & Sons.
Webster, R., 2001. Statistics to support soil research and their presentation. J. Soil Sci. 52, 331–340.
Weier, K.L., Doran, J.W., Power, J.F., Walters, D.T., 1993. Denitrification and the dinitrogen/nitrous oxide ratio as affected by soil water, available carbon, and nitrate. Soil Sci. Soc. Am. J. 57, 66–72.
Weitz, A.M., Keller, M., Linder, E., Crill, P.M., 1999. Spatial and temporal variability of nitrogen oxide and methane fluxes from a fertilized tree plantation in Costa Rica. J. Geophys. Res. Atmos. 104, 30097–30107. doi:http://dx.doi.org/10.1029/1999JD900952.
Whelan, B.M., McBratney, A.B., 2003. Definition and interpretation of potential management zones. Australia Proceedings of the 11th Australian Agronomy Conference 2–6.
Wickings, K., Grandy, A.S., Kravchenko, A.N., 2016. Going with the flow: landscape position drives differences in microbial biomass and activity in conventional, low input, and organic agricultural systems in the Midwestern U.S. Agric. Ecosyst. Environ. 218, 1–10. doi:http://dx.doi.org/10.1016/j.agee.2015.11.005.
Wilford, J., Minty, B., 2006. The use of airborne gamma-ray imagery for mapping soils and understanding landscape processes. In: Lagacherie, P., McBratney, A.B., Voltz, M. (Eds.), Developments in Soil Science. Elsevier, pp. 609–610.
Yanai, J., Sawamoto, T., Oe, T., Kusa, K., Yamakawa, K., Sakamoto, K., Naganawa, T., Inubushi, K., Hatano, R., Kosaki, T., 2003. Spatial variability of nitrous oxide emissions and their soil-related determining factors in an agricultural field. J. Environ. Qual. 32, 1965–1977. doi:http://dx.doi.org/10.2134/jeq2003.1965.
Zhu, Q., Lin, H., Doolittle, J., 2010. Repeated electromagnetic induction surveys for improved soil mapping in an agricultural landscape. Soil Sci. Soc. Am. J. 74, 1763–1774.